

Asymmetrical magnetic domain wall motion in symmetrical heavy metal/ferromagnet multilayersMaokang Shen,^{1,2,*} Xiangyu Li,^{2,*} Long You,² Xiaofei Yang,² Wei Luo,² and Yue Zhang^{2,†}¹*School of Physics and Optoelectronics, Xiangtan University, Xiangtan, China*²*School of Optical and Electronic Information, Huazhong University of Science and Technology, Wuhan, China*

(Received 18 October 2021; revised 20 February 2022; accepted 13 April 2022; published 27 April 2022)

In a heavy metal (HM)/ferromagnet (FM)/HM multilayer with a symmetrical sandwich structure, the absence of an interfacial Dzyaloshinskii-Moriya interaction (iDMI) is generally expected. A zero iDMI constant is usually verified by the motion of a magnetic domain wall (DW) with a velocity that is symmetrical to the longitudinal magnetic field (symmetrical DW motion). However, asymmetrical DW motion was still experimentally observed in a symmetrical HM/FM/HM multilayer, and its mechanism is unclear. In this letter, we theoretically prove that even in a *perfectly* symmetrical HM/FM/HM multilayer with a zero total iDMI constant, asymmetrical DW motion is still possible owing to the exchange coupling between the neighboring FM atomic layers in the FM medium. This work paves a way to unraveling unique DW motion in HM/FM multilayers from a deep perspective of the subtle magnetic interactions within a FM medium.

DOI: [10.1103/PhysRevB.105.L140402](https://doi.org/10.1103/PhysRevB.105.L140402)

Motion of a magnetic domain wall (DW) plays a crucial role in developing novel magnetic memory and logic devices [1–5]. The DW in a heavy metal (HM)/ferromagnet (FM) multilayer with broken inversion symmetry exhibits a chiral structure owing to the interfacial Dzyaloshinskii-Moriya interaction (iDMI) [6–10]. The iDMI depresses Walker breakdown and assists fast DW motion driven by spin-orbit torque [6,9,11–14]. Since the iDMI is taken as an effective longitudinal magnetic field (H_{DM}) along the direction for DW motion, the DW velocity is asymmetrical to the external longitudinal magnetic field in the presence of an iDMI (asymmetrical DW motion) [14–16].

In principle, the absence of iDMI and symmetrical DW motion is expected in a HM/FM/HM multilayer with inversion symmetry—i.e., the HM layers above and below the FM layer share the same composition and thickness. Yet, asymmetrical DW motion was still widely observed in such a symmetrical HM/FM/HM multilayer [17–22]. This can be attributed to experimental factors. For example, the microscopic lattice structure may be not equal for the bottom FM/HM and top HM/FM interfaces [23,24]. Also, the bottom FM/HM and top HM/FM interfaces can be unequally strained [19], which may influence the iDMI [25,26]. Additionally, the pinning effect may also modify the DW velocity as a function of H_x [27].

All these factors make sense for explaining the unexpected asymmetrical DW motion in experiments. In a *strictly* symmetrical HM/FM/HM multilayer in the absence of these extrinsic factors, one may be confident of observing symmetrical DW motion. Nevertheless, this expectation is still questionable if the magnetic interaction *in* the FM medium is carefully considered. Unlike a two-dimensional material with

only one atomic layer, the FM medium in a HM/FM multilayer contains at least two to three atomic layers [24,27,28]. In such a symmetrical HM/FM/HM multilayer, even if the total iDMI constant is zero, the *local* iDMI constants for the top and bottom FM atomic layers can be still nonzero, owing to their local asymmetrical surroundings. This local iDMI is not negligible since DMI has a dominant contribution from the neighboring atomic layers at the HM/FM interface [24,28,29]. In addition to the local iDMI, there is also exchange coupling between the neighboring atomic layers in a FM medium (Fig. 1). However, in a previous calculation, the FM medium in an ultrathin HM/FM multilayer is usually simplified as a single atomic layer, and the influence of the slight magnetic interactions in the FM medium on DW motion has not been taken into account.

In this Letter, based on theoretical and numerical investigation, we show that besides iDMI, the exchange coupling between the neighboring atomic layers in a FM medium also plays a crucial role in asymmetrical DW motion. Even in a strictly symmetrical HM/FM/HM multilayer with a zero total iDMI constant, this exchange coupling still gives rise to asymmetrical DW motion. This unravels an *intrinsic* mechanism for asymmetrical DW motion in a symmetrical HM/FM multilayer.

We consider magnetic-field-induced DW motion in a HM/FM/HM multilayer with symmetrical sandwich structure (Fig. 1). For simplicity, we assume the FM medium contains two atomic layers, and the two HM layers above and below the FM medium are exactly the same. Owing to the opposite sequence of the HM and FM layers, the local iDMI constants of the bottom HM/FM layer (D_b) and the top FM/HM layer (D_t) are opposite ($D_b = -D_t$). The ferromagnetic exchange coupling exists in a FM atomic layer and between the neighboring FM atomic layers.

A theoretical investigation about the dynamics of a magnetic texture can be traced back to Thiele’s original works

*These authors contributed equally to this work.

†yue-zhang@hust.edu.cn

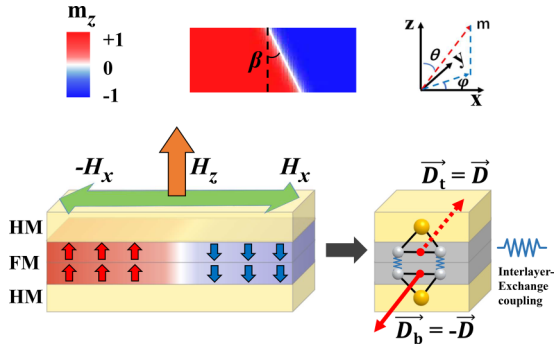


FIG. 1. Schematic of the magnetic-field-induced DW motion in a HM/FM/HM multilayer with a symmetrical structure. The FM medium is composed of two atomic layers, and the bottom and top HM layers share the same composition and thickness. An opposite local iDMI appears at the bottom HM/FM layer and the top FM/HM layer, with an exchange coupling between the two FM atomic layers. The DW is driven by an out-of-plane magnetic field (H_z) and a longitudinal magnetic field along the positive and negative x direction ($\pm H_x$). The azimuthal angle φ and the DW tilting angle β are as indicated.

[30,31]. In our calculation, the DW dynamics with iDMI is depicted by the collective coordinate method, where the DW is described by three independent variables [32]: the central position (q), the azimuthal angle (φ) of the magnetization at the central DW, and the tilting angle (β) of the DW plane (Fig. 1). We assume moderate exchange coupling between the FM atomic layers, which gives rise to synchronous motion of the coupled DWs—i.e., the two DWs have identical q and β .

The derivation of DW dynamics equations starts with a uniform magnetization vector $\vec{m}_{b(t)} = (\sin \theta \cos \varphi_{b(t)}, \sin \theta \sin \varphi_{b(t)}, \cos \theta)$, where θ and φ are a polar angle and an azimuthal angle with the subscript b and t representing the bottom and top FM atomic layers, respectively. The DW profiles in the two FM atomic layers are expressed as [30]: $\theta_b = \theta_t = 2 \arctan\{\exp[(x \cos \beta + y \sin \beta - q)/\Delta]\}$, with Δ representing the DW width.

The energy density (w) of a multilayer consists of the contributions from the bottom and top FM atomic layers (w_b

and w_t) and the coupling between them (w_{b-t}): $w = w_b + w_t + w_{b-t}$. These energy densities are written as

$$w_{b(t)} = \frac{A}{\Delta^2} \sin^2 \theta + \left(K - \frac{1}{2} \mu_0 M_S^2 \right) \sin^2 \theta + \frac{1}{2} \mu_0 N_x M_S^2 \sin^2 \theta \cos^2(\varphi_{b(t)} - \beta) + \frac{D_{b(t)} \sin \theta \cos(\varphi_{b(t)} - \beta)}{\Delta} - \mu_0 M_S H_z \cos \theta - \mu_0 M_S H_x \sin \theta \cos \varphi_{b(t)} \quad (1)$$

and

$$w_{b-t} = -\frac{\sigma}{t_s^2} [\sin^2 \theta \cos(\varphi_b - \varphi_t) + \cos^2 \theta]. \quad (2)$$

Here t_s , σ , A , K , D , M_S , H_z , and H_x are the distance between the two FM atomic layers, the exchange constant between the neighboring FM atomic layers and inner an FM atomic layer, the anisotropy constant, the iDMI constant, the saturation magnetization, and the magnetic-field strength along the z and x directions, respectively. N_x is the demagnetization factor. Based on the method proposed by Tarasenko *et al.* [33], the N_x of a Néel-type DW in an ultrathin FM film with iDMI can be approximated as $N_x \approx L_z \ln 2/\pi \Delta$, where L_z is the FM-layer thickness [6,10,34–38].

The Lagrangian density function (l) and the dissipation density function (f) of the multilayer can be expressed as [32]

$$l = w + \frac{M_S}{\gamma} \varphi_t \dot{\theta}_t \sin \theta_t + \frac{M_S}{\gamma} \varphi_b \dot{\theta}_b \sin \theta_b \quad (3)$$

and

$$f_d = (\alpha M_S / 2\gamma) [(d\vec{m}_t/dt)^2 + (d\vec{m}_b/dt)^2]. \quad (4)$$

In Eqs. (3) and (4), α and γ are the Gilbert damping coefficient and the gyromagnetic ratio of an electron ($\gamma = 1.76 \times 10^{11} \text{ T}^{-1} \text{ s}^{-1}$), respectively.

The Lagrangian function (L) and the dissipation function (F) were established by integrating l and f with respect to the entire multilayer space:

$$L = \int_0^{t_m} \int_{-\frac{d}{2}}^{\frac{d}{2}} \int_{-\infty}^{+\infty} l dx dy dz = \frac{4Adt_m}{\Delta \cos \beta} - \frac{dt_m M_S \varphi_t \dot{q}}{\gamma} - \frac{dt_m M_S \varphi_b \dot{q}}{\gamma} + \frac{\Delta dt_m \mu_0 N_x M_S^2 \cos^2(\varphi_t - \beta)}{2 \cos \beta} + \frac{\Delta dt_m \mu_0 N_x M_S^2 \cos^2(\varphi_b - \beta)}{2 \cos \beta} + \frac{dt_m D_t \pi \cos(\varphi_t - \beta)}{2 \cos \beta} + \frac{dt_m D_b \pi \cos(\varphi_b - \beta)}{2 \cos \beta} - 2dt_m q \mu_0 M_S H_z - \frac{\Delta \pi dt_m}{2 \cos \beta} M_S H_x \cos \varphi_t - \frac{\Delta \pi dt_m}{2 \cos \beta} M_S H_x \cos \varphi_b - \frac{2\Delta dt_m \sigma}{t_s^2} \cos(\varphi_b - \varphi_t) \quad (5)$$

and

$$F = \int_0^{t_m} \int_{-\frac{d}{2}}^{\frac{d}{2}} \int_{-\infty}^{+\infty} f_d dx dy dz = \frac{\alpha M_S dt_m}{2\gamma} \left\{ \frac{2 \cos \beta (\dot{q})^2}{\Delta} + \frac{\Delta [(\dot{\varphi}_t)^2 + (\dot{\varphi}_b)^2]}{\cos \beta} + \left(\frac{\Delta \pi^2 \sin^2 \beta}{6 \cos^3 \beta} + \frac{d^2}{6 \Delta \cos^3 \beta} \right) (\dot{\beta})^2 \right\}. \quad (6)$$

The L and F were then plugged into the Lagrange-Rayleigh equation:

$$\frac{\partial L}{\partial q_i} - \frac{d}{dt} \left(\frac{\partial L}{\partial \dot{q}_i} \right) + \frac{\partial F}{\partial \dot{q}_i} = 0. \quad (7)$$

Here, $q_i = q, \varphi_t, \varphi_b$, and β . After algebraic computing, we finally derived the Thiele equations:

$$\frac{4\alpha \cos \beta}{\Delta} \dot{q} + \dot{\varphi}_b + \dot{\varphi}_t = 2\gamma_0 H_z, \quad (8)$$

$$\begin{aligned} \frac{\cos \beta}{\Delta} \dot{q} - \alpha \dot{\varphi}_b &= \frac{\gamma_0 \pi D_b \sin(\varphi_b - \beta)}{2\Delta \mu_0 M_S} + \frac{\gamma_0 N_x M_S \sin[2(\varphi_b - \beta)]}{2} \\ &+ \frac{2\sigma \gamma_0 \sin(\varphi_b - \varphi_t)}{\mu_0 M_S t_s^2} + \frac{\gamma_0 \pi H_x \sin \varphi_b}{2}, \end{aligned} \quad (9)$$

$$\begin{aligned} \frac{\cos \beta}{\Delta} \dot{q} - \alpha \dot{\varphi}_t &= \frac{\gamma_0 \pi D_t \sin(\varphi_t - \beta)}{2\Delta \mu_0 M_S} + \frac{\gamma_0 N_x M_S \sin[2(\varphi_t - \beta)]}{2} \\ &- \frac{2\sigma \gamma_0 \sin(\varphi_b - \varphi_t)}{\mu_0 M_S t_s^2} + \frac{\gamma_0 \pi H_x \sin \varphi_t}{2}, \end{aligned} \quad (10)$$

and

$$\begin{aligned} \frac{\pi^2 \Delta \alpha \mu_0 M_S}{3\gamma_0} \left[\tan^2 \beta + \left(\frac{w}{\pi \Delta} \right)^2 \frac{1}{\cos^2 \beta} \right] \dot{\beta} &= - \left\{ \Delta \mu_0 N_x M_S^2 \sin[2(\varphi_b - \beta)] \right. \\ &+ \Delta \mu_0 N_x M_S^2 \cos^2(\varphi_b - \beta) \tan \beta + \frac{8A}{\Delta} \tan \beta \\ &- \left. \frac{\pi D_b \sin \varphi_b}{\cos \beta} - \Delta \pi \mu_0 H_x M_S \cos \varphi_b \tan \beta \right\} \\ &- \left\{ \Delta \mu_0 N_x M_S^2 \sin[2(\varphi_t - \beta)] \right. \\ &+ \Delta \mu_0 N_x M_S^2 \cos^2(\varphi_t - \beta) \tan \beta - \frac{\pi D_t \sin \varphi_t}{\cos \beta} \\ &- \left. \Delta \pi \mu_0 H_x M_S \cos \varphi_t \tan \beta \right\}. \end{aligned} \quad (11)$$

At a stable state ($\dot{\varphi}_b = \dot{\varphi}_t = \dot{\beta} = 0$) without Walker breakdown, Eq. (8) is converted to

$$\dot{q} = \frac{\gamma_0 H_z \Delta}{2\alpha \cos \beta}. \quad (12)$$

This indicates that stable DW velocity relies on H_z and β .

Equations (8)–(11) were numerically solved by the fourth-order Runge–Kutta–Fehlberg method (time step, 100 ps). We consider a perpendicularly magnetized Pt/CoFeB/Pt multilayer [39–44]. The magnetic parameters of a bulk CoFeB can be $K = 8 \times 10^5 \text{ J/m}^3$, $A = 1 \times 10^{-11} \text{ J/m}$, and $M_S = 1.2 \times 10^6 \text{ A/m}$ [45]. In this work, we reduced the previous A and M_S by half due to a dead magnetic layer in an ultrathin film; σ is around A , and the α of an ultrathin CoFeB film is 0.01 [46–48].

The iDMI constant of Pt/CoFeB can be 1 mJ/m^2 or larger [49,50]. The local iDMI constant of a single CoFeB atomic layer adherent to Pt has not been reported. However, we can still estimate it based on the reported *ab initio* calculation about the iDMI of Pt/Co and Pt/Fe. Yang *et al.* [28] show that the iDMI constant of a Pt/Co system with two Co atomic layers can be 4 to 5 mJ/m^2 , and the Co atom adherent to Pt plays a dominant role in the iDMI, while the iDMI constant of Pt/Fe is much smaller [51,52]. Therefore, in a CoFeB system composed of Co and Fe with identical atomic numbers, such as $\text{Co}_{40}\text{Fe}_{40}\text{B}_{20}$, the local iDMI constant for an atomic layer adherent to Pt can be 2 to 3 mJ/m^2 .

Before solving Eqs. (8)–(11), we first estimated DW motion by analyzing the symmetry of the equations. For a single FM atomic layer without iDMI, the DW velocity is symmetrical to H_x . At a nonzero iDMI constant, however, the DW velocity becomes asymmetrical to H_x since the iDMI can be taken as an effective longitudinal magnetic field (H_{DM}) [15]. However, the magnitude of the total longitudinal magnetic field under H_x for D is still the same as that under $-H_x$ for $-D$, and the DW tilting under H_x for D is identical to that under $-H_x$ for $-D$. Therefore, in a symmetrical HM/FM/HM multilayer with two FM atomic layers *without interlayer exchange coupling*, the coexistence of D and $-D$ still keeps the symmetry of DW motion under $\pm H_x$. [The DW motion for (H_x, D) is symmetrical to that for $(-H_x, -D)$; the DW motion for $(H_x, -D)$ is symmetrical to that for $(-H_x, D)$.] This can be confirmed from the symmetry of Eqs. (9) and (10) with a zero σ . Nevertheless, a nonzero σ breaks this symmetry, and the DW motion for (H_x, D) becomes asymmetrical to that for $(-H_x, -D)$.

To solve Eqs. (8)–(11), we first determined the stable DW structure as the initial condition. Initially, $q_0 = 0$ and $\beta_0 = 0$, and the equilibrium DW structure is between a Bloch type and a Néel type due to the tradeoff between opposite local iDMI constants at two FM atomic layers and the interlayer exchange coupling. Quantitatively, φ_{b0} and φ_{t0} can be derived by minimizing w for $\theta = \pi/2$ (the magnetization at the central DW) under the condition $|\varphi_{b0} + \varphi_{t0}| = \pi$ due to symmetry, and φ_{t0} and φ_{b0} satisfies

$$|\cos \varphi_{t0}| = |\cos \varphi_{b0}| = \left| \frac{D_t}{\Delta(\mu_0 N_x M_S^2 + \frac{2\sigma}{t_s^2})} \right|, \quad (13)$$

where $||$ is the symbol for an absolute value.

Based on the previous initial conditions, the dynamics of DW variables were numerically solved ($\sigma = 5 \times 10^{-12} \text{ J/m}$). Under H_z , the DW moves at a velocity manipulated by H_x . When the FM medium contains only one atomic layer with a zero iDMI constant, the DW velocity is symmetrical to H_x and reaches a flat when H_x exceeds about 700 Oe due to transition of the initial DW structure from a Bloch DW to a Néel DW [Fig. 2(a)]. Nevertheless, for a FM medium containing two atomic layers with opposite local iDMI constants, the DW velocity becomes asymmetrical to H_x [Fig. 2(b)]. Under $H_z = 10(-10)$ Oe, the H_x for the minimum DW velocity is around 700 (–700) Oe. To clarify the relationship between asymmetrical DW velocity and DW tilting, we derived the DW tilting angle under H_x . In a FM medium composed of two atomic layers, $\beta(H_x)$ is different from $\beta(-H_x)$ [Fig. 2(c)]. However,

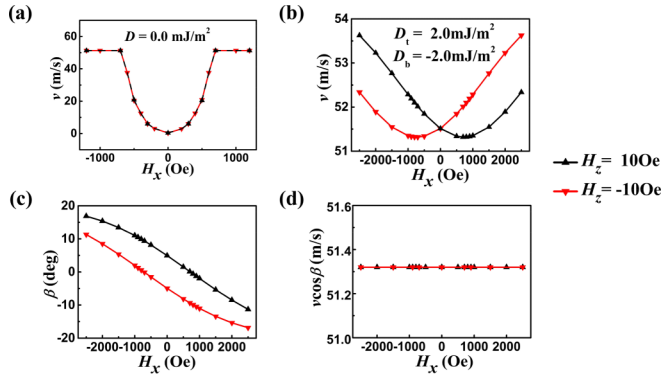


FIG. 2. (a) DW velocity as a function of H_x for the HM/FM/HM multilayer with a single FM atomic layer and zero iDMI. (b) DW velocity as a function of H_x for the HM/FM/HM multilayer composed of two FM atomic layers with opposite iDMI constants. (c) DW tilting angle β as a function of H_x for the HM/FM/HM multilayer. (d) Product of DW velocity and $\cos\beta$ as a function of H_x .

the product of DW velocity and $\cos\beta$ is still independent of H_x , which satisfies the prediction by Eq. (12) [Fig. 2(d)].

The difference of DW velocity under $\pm H_x$ (Δv) is manipulated by different parameters (Fig. 3). Δv exhibits nonmonotonous variation with H_x , reaching a maximum value around $H_x = 2000$ Oe [Fig. 3(a)]. At a very high H_x , the iDMI becomes negligible compared to H_x , which leads to a reduction in Δv . The difference of DW velocity significantly increases with an increasing local iDMI constant, with a critical D around 1.5 mJ/m², below which Δv is zero [Fig. 3(b)]. Similarly, there is also a critical σ around 3 pJ/m, below which the DW motions of the two layers are decoupled, and Δv gradually decreases with increasing σ above this critical value [Fig. 3(c)]. Under very strong interlayer exchange coupling, the iDMI-induced DW tilting is inhibited, which results in the disappearance of Δv .

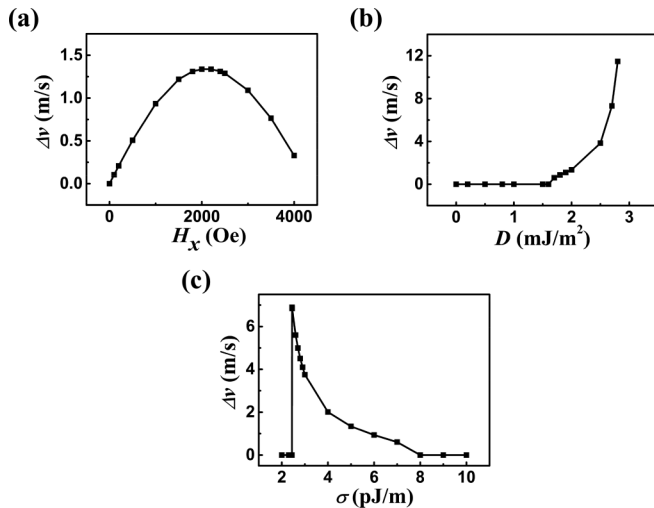


FIG. 3. (a) Difference of DW velocity as a function of H_x . (b) Difference of DW velocity as a function of the iDMI constant. (c) Difference of DW velocity as a function of the interlayer exchange constant.

The theoretical results were verified using Object-Oriented-Micro-Magnetic-Framework software based on numerically solving the Landau–Lifshitz–Gilbert equation:

$$\frac{\partial \vec{m}_{b(t)}}{\partial t} = -\gamma_0 \vec{m}_{b(t)} \times \vec{H}_{\text{eff},b(t)} + \alpha \vec{m}_{b(t)} \times \frac{\partial \vec{m}_{b(t)}}{\partial t}. \quad (14)$$

Here, the effective magnetic field was calculated by the functional derivative as $\vec{H}_{\text{eff}} = -\frac{1}{\mu_0 M_S} \frac{\delta E}{\delta \vec{m}}$, with E as the energy functional $E = \int_V w d\tau$. The model and its dimension are illustrated in Fig. 4(a). We considered a FM medium with a single atomic layer (left), and that with two coupled atomic layers (right). The size of the unit cell is $1 \times 1 \times 0.4$ nm, which is obviously smaller than the exchange length ($l_{\text{ex}} = 4.8$ nm as estimated by $l_{\text{ex}} = \sqrt{2A/\mu_0 M_S^2}$). Since we considered a symmetrical HM/FM/HM multilayer, zero D was assumed for the single atomic layer, and two opposite D values ($D_t = -D_b$) were considered for the two coupled atomic layers.

Initially, the DW structure in the single layer is a Bloch type, while that in the two coupled layers is between a Néel type and a Bloch type [Figs. 4(b)–4(d)]. In the single layer, $D = 0$ mJ/m². In the coupled layers, the absolute values of $\cos\varphi_{b0}$ and $\cos\varphi_{l0}$ for $D_t = 2.0$ mJ/m² and $D_b = -2.0$ mJ/m² are both 0.0274 , and that for $D_t = 5.0$ mJ/m² and $D_b = -5.0$ mJ/m² are 0.0686 . The simulated results are close to those calculated by Eq. (13) (0.0276 for $D_t = 2.0$ mJ/m² and $D_b = -2.0$ mJ/m², and 0.0732 for $D_t = 5.0$ mJ/m² and $D_b = -5.0$ mJ/m²).

The profiles and the stable velocities of the DWs under positive and negative H_x are also exhibited in Figs. 4(b)–4(d). In a single FM atomic layer with a zero D , the DW magnetization under $H_x = 2000$ Oe is antiparallel to that under $H_x = -2000$ Oe, and the DW velocity under H_x is the same as that under $-H_x$ [Fig. 4(b)]. In the FM medium with two coupled atomic layers, owing to the exchange coupling between the two atomic layers, the DW magnetizations in the two layers are almost the same, but the DW magnetization for $H_x = 2000$ Oe is asymmetrical to that for $H_x = -2000$ Oe. This gives rise to different DW tilting angles and DW velocity for $H_x = \pm 2000$ Oe [Figs. 4(c) and 4(d)].

The simulated results are close to the numerical solutions of the Thiele equations (Fig. 2) under a smaller σ for the simulation ($\sigma = 2 \times 10^{-12}$ J/m). This difference between the simulation and theory can be attributed to the error in estimating the demagnetizing energy in solving the Thiele equations and the influence of the iDMI boundary effect in the simulation [53].

Finally, we briefly discuss about how to confirm the theoretical prediction in experiments. The trick is the fabrication of a HM/FM/HM multilayer with two HM layers sharing very similar composition and thickness. To avoid inhomogeneous strain, one may synthesize two additional layers below the bottom HM layer and above the top one, and it may be better to fabricate the multilayers using molecular-beam epitaxy that can precisely control the growth of each atomic layer.

In summary, we propose an intrinsic mechanism for understanding the asymmetrical DW motion in symmetrical HM/FM/HM multilayers by considering the magnetic inter-

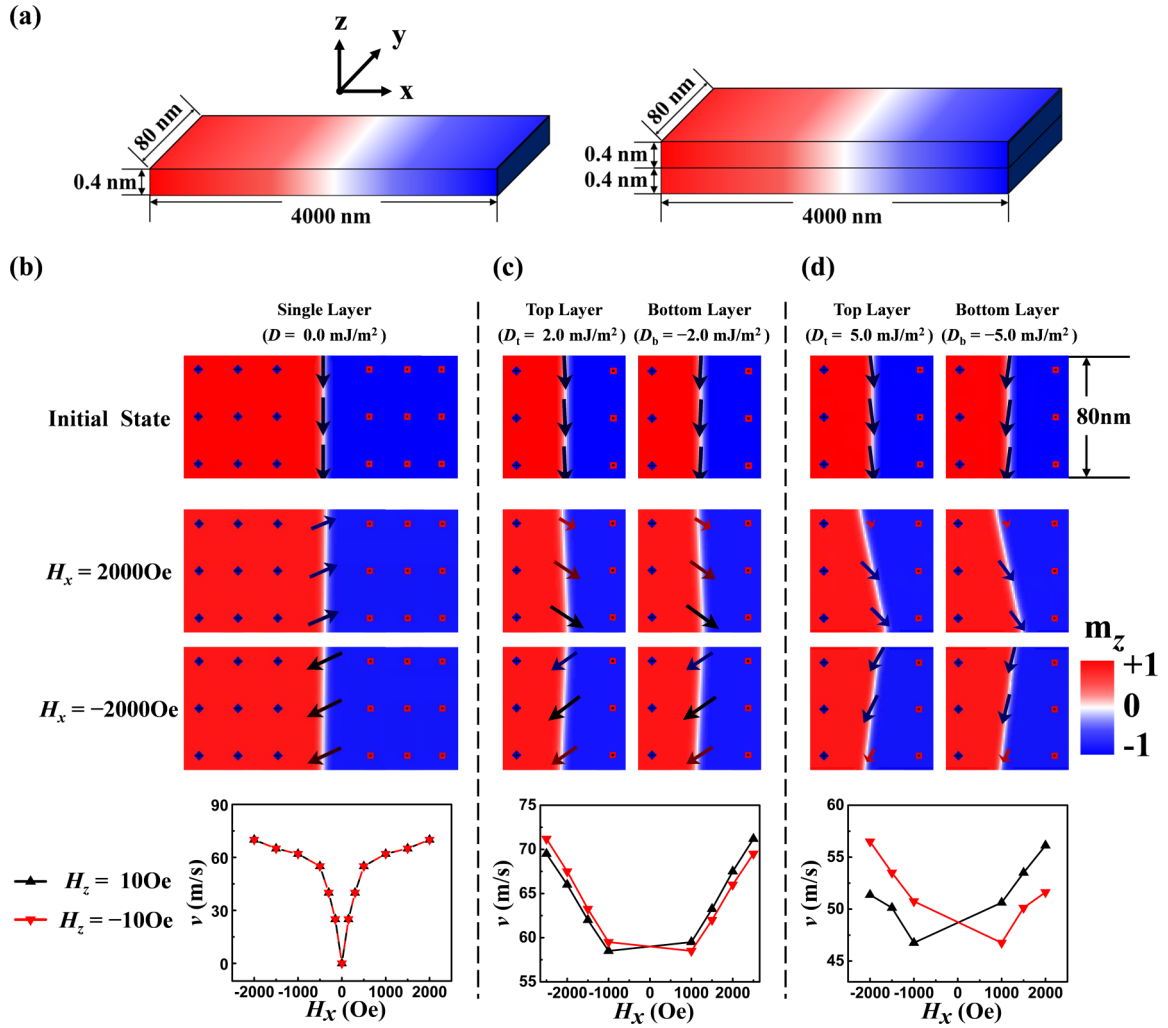


FIG. 4. Simulated DW profiles and DW velocity as a function of H_x for a symmetrical HM/FM/HM multilayer. (a) The dimension of the models for the simulation, including a single FM atomic layer (left) and a FM medium composed of two coupled atomic layers (right). (b) The DW profile in a single FM atomic layer with zero iDMI. (c) The DW profile in a FM medium composed of two atomic layers with $D_t = 2.0 \text{ mJ/m}^2$ and $D_b = -2.0 \text{ mJ/m}^2$. (d) The DW profile in a FM medium composed of two FM atomic layers with $D_t = 5.0 \text{ mJ/m}^2$ and $D_b = -5.0 \text{ mJ/m}^2$. In (b), (c), and (d), the profiles of the DWs at the initial state and under $H_x = \pm 2000 \text{ Oe}$ are presented. The dots and arrows indicate the orientation of the unit magnetization vector in a cell. (The blue and red dots show the unit magnetization vector aligning along z and $-z$ directions.)

action *within* a FM medium. We show that the exchange coupling between the neighboring FM atomic layers destroys the symmetry for DW tilting under $\pm H_x$, giving rise to asymmetrical DW motion in HM/FM/HM multilayers with a strictly symmetrical structure. This work paves the way for deep exploration of the motion of a chiral DW in a HM/FM multilayer system from the

perspective of subtle magnetic interactions within a FM medium.

The authors acknowledge financial support from the National Key Research and Development Program of China (Grant No. 2022YFE0103300) and the National Natural Science Foundation of China (Grant No. 51971098).

[1] S. S. P. Parkin, M. Hayashi, and L. Thomas, *Science* **320**, 190 (2008).
 [2] R. Bläsing, A. A. Khan, P. C. Filippou, C. Garg, F. Hameed, J. Castrillon, and S. S. P. Parkin, *Proc. IEEE* **108**, 1303 (2020).
 [3] D. A. Allwood, G. Xiong, C. C. Faulkner, D. Atkinson, D. Petit, and R. P. Cowburn, *Science* **309**, 1688 (2005).

[4] Z. Luo, A. Hrabec, T. P. Dao, G. Sala, S. Finizio, J. Feng, S. Mayr, J. Raabe, P. Gambardella, and L. J. Heyderman, *Nature (London)* **579**, 214 (2020).
 [5] G. Catalan, J. Seidel, R. Ramesh, and J. F. Scott, *Rev. Mod. Phys.* **84**, 119 (2012).
 [6] A. Thiaville, S. Rohart, E. Jué, V. Cros, and A. Fert, *Europhys. Lett.* **100**, 57002 (2012).

- [7] S. Emori, U. Bauer, S.-M. Ahn, E. Martinez, and G. S. D. Beach, *Nat. Mater.* **12**, 611 (2013).
- [8] K.-S. Ryu, L. Thomas, S.-H. Yang, and S. Parkin, *Nat. Nanotech.* **8**, 527 (2013).
- [9] R. Tomasello, V. Puliafito, E. Martinez, A. Manchon, M. Ricci, M. Carpentieri, and G. Finocchio, *J. Phys. D Appl. Phys.* **50**, 325302 (2017).
- [10] S. Emori, E. Martinez, K.-J. Lee, H.-W. Lee, U. Bauer, S.-M. Ahn, P. Agrawal, D. C. Bono, and G. S. D. Beach, *Phys. Rev. B* **90**, 184427 (2014).
- [11] J. Lucassen, C. F. Schippers, M. A. Verheijen, P. Fritsch, E. J. Geluk, B. Barcones, R. A. Duine, S. Wurmehl, H. J. M. Swagten, B. Koopmans, and R. Lavrijsen, *Phys. Rev. B* **101**, 064432 (2020).
- [12] R. M. Rowan-Robinson, A. A. Stashkevich, Y. Roussigné, M. Belmeguenai, S.-M. Chérif, A. Thiaville, T. P. A. Hase, A. T. Hindmarch, and D. Atkinson, *Sci. Rep.* **7**, 16835 (2017).
- [13] C. Moreau-Luchaire *et al.*, *Nat. Nanotech.* **11**, 444 (2016).
- [14] F. Ajejas, V. Kžáková, D. D. S. Chaves, J. Vogel, P. Perna, R. Guerrero, A. Gudin, J. Camarero, and S. Pizzini, *Appl. Phys. Lett.* **111**, 202402 (2017).
- [15] E. Jué *et al.*, *Phys. Rev. B* **93**, 014403 (2016).
- [16] P. M. Shepley, H. Tunnickliffé, K. Shahbazi, G. Burnell, and T. A. Moore, *Phys. Rev. B* **97**, 134417 (2018).
- [17] S.-G. Je, D.-H. Kim, S.-C. Yoo, B.-C. Min, K.-J. Lee, and S.-B. Choe, *Phys. Rev. B* **88**, 214401 (2013).
- [18] R. Lavrijsen, D. M. F. Hartmann, A. van den Brink, Y. Yin, B. Barcones, R. A. Duine, M. A. Verheijen, H. J. M. Swagten, and B. Koopmans, *Phys. Rev. B* **91**, 104414 (2015).
- [19] A. V. Davydenko, A. G. Kozlov, M. E. Stebliy, A. G. Kolesnikov, N. I. Sarnavskiy, I. G. Iliushin, and A. P. Golikov, *Phys. Rev. B* **103**, 094435 (2021).
- [20] B. Zhang, Y. Xu, W. Zhao, D. Zhu, H. Yang, X. Lin, M. Hehn, G. Malinowski, N. Vernier, D. Ravelosona, and S. Mangin, *Phys. Rev. B* **99**, 144402 (2019).
- [21] K. Shahbazi, A. Hrabec, S. Moretti, M. B. Ward, T. A. Moore, V. Jeudy, E. Martinez, and C. H. Marrows, *Phys. Rev. B* **98**, 214413 (2018).
- [22] K.-J. Kim, Y. Yoshimura, T. Okuno, T. Moriyama¹, S.-W. Lee, K.-J. Lee, Y. Nakatani, and T. Ono, *APL Mater.* **4**, 032504 (2016).
- [23] A. V. Davydenko, A. G. Kozlov, A. G. Kolesnikov, M. E. Stebliy, G. S. Suslin, Y. E. Vekovshinin, A. V. Sadovnikov, and S. A. Nikitov, *Phys. Rev. B* **99**, 014433 (2019).
- [24] W. Zhang, R. Chen, B. Jiang, X. Zhao, W. Zhao, S. S. Yan, G. Han, S. Yu, G. Liu, and S. Kang, *Nanoscale* **13**, 2665 (2021).
- [25] C. Deger, *Sci. Rep.* **10**, 12314 (2020).
- [26] N. S. Gusev, A. V. Sadovnikov, S. A. Nikitov, M. V. Sapozhnikov, and O. G. Udalov, *Phys. Rev. Lett.* **124**, 157202 (2020).
- [27] K. Shahbazi, J.-V. Kim, H. T. Nembach, J. M. Shaw, A. Bischof, M. D. Rossell, V. Jeudy, T. A. Moore, and C. H. Marrows, *Phys. Rev. B* **99**, 094409 (2019).
- [28] H. Yang, A. Thiaville, S. Rohart, A. Fert, and M. Chshiev, *Phys. Rev. Lett.* **115**, 267210 (2015).
- [29] O. G. Udalov and I. S. Beloborodov, *Phys. Rev. B* **102**, 134422 (2020).
- [30] A. A. Thiele, *Phys. Rev. Lett.* **30**, 230 (1973).
- [31] A. A. Thiele, *J. Appl. Phys.* **45**, 377 (1974).
- [32] O. Boulle, S. Rohart, L. D. Buda-Prejbeanu, E. Jué, I. M. Miron, S. Pizzini, J. Vogel, G. Gaudin, and A. Thiaville, *Phys. Rev. Lett.* **111**, 217203 (2013).
- [33] S. V. Tarasenko, A. Stankiewicz, V. V. Tarasenko, and J. Ferré, *J. Magn. Magn. Mater.* **189**, 19 (1998).
- [34] A. Hrabec, N. A. Porter, A. Wells, M. J. Benitez, G. Burnell, S. McVitie, D. McGrouther, T. A. Moore, and C. H. Marrows, *Phys. Rev. B* **90**, 020402(R) (2014).
- [35] M. J. Benitez, A. Hrabec, A. P. Mihai, T. A. Moore, G. Burnell, D. McGrouther, C. H. Marrows, and S. McVitie, *Nat. Commun.* **6**, 8957 (2015).
- [36] R. L. Conte *et al.*, *Phys. Rev. B* **91**, 014433 (2015).
- [37] L. Caretta, E. Rosenberg, F. Büttner, T. Fakhrlul, P. Gargiani, M. Valvidares, Z. Chen, P. Reddy, D. A. Muller, C. A. Ross, and G. S. D. Beach, *Nat. Commun.* **11**, 1090 (2020).
- [38] E. Martinez, S. Emori, N. Perez, L. Torres, and G. S. D. Beach, *J. Appl. Phys.* **115**, 213909 (2014).
- [39] J. Wells, J. H. Lee, R. Mansell, R. P. Cowburn, and O. Kazakova, *J. Magn. Magn. Mater.* **400**, 219 (2016).
- [40] S. B. Wu, X. F. Yang, S. Chen, and T. Zhu, *J. Appl. Phys.* **113**, 17C119 (2013).
- [41] J. Cho, N.-H. Kim, S. K. Kang, H.-K. Hwang, J. Jung, H. J. M. Swagten, J.-S. Kim, and C.-Y. You, *J. Phys. D Appl. Phys.* **50**, 425004 (2017).
- [42] J. Wells, A. F. Scarioni, H. W. Schumacher, D. Cox, R. Mansell, R. Cowburn, and O. Kazakova, *AIP Adv.* **7**, 056715 (2017).
- [43] P. Krzysteczko *et al.*, *Phys. Rev. B* **95**, 220410(R) (2017).
- [44] Y. Zhu, Z. Zhang, B. Ma, and Q. Y. Jin, *J. Appl. Phys.* **111**, 07C106 (2012).
- [45] Z. Yu *et al.*, *Nanoscale Adv.* **2**, 1309 (2020).
- [46] D. M. Lattery, D. Zhang, J. Zhu, X. Hang, J.-P. Wang, and X. Wang, *Sci. Rep.* **8**, 13395 (2018).
- [47] S. Iihama, Q. Ma, T. Kubota, S. Mizukami, Y. Ando, and T. Miyazaki, *Appl. Phys. Express* **5**, 083001 (2012).
- [48] S. Iihama, S. Mizukami, H. Naganum, M. Oogane, Y. Ando, and T. Miyazaki, *Phys. Rev. B* **89**, 174416 (2014).
- [49] K. Di, V. L. Zhang, H. S. Lim, S. C. Ng, M. H. Kuok, X. Qiu, and H. Yang, *Appl. Phys. Lett.* **106**, 052403 (2015).
- [50] T. Böttcher, K. Lee, F. Heussner, S. Jaiswal, G. Jakob, M. Kläui, B. Hillebrands, T. Brächer, and P. Pirro, *IEEE Trans. Magn.* **57**, 1600207 (2021).
- [51] S. Mankovsky, E. Simon, S. Polesya, A. Marmodoro, and H. Ebert, *Phys. Rev. B* **104**, 174443 (2021).
- [52] M. Schott, L. Ranno, H. Béa, C. Baraduc, S. Auffret, and A. Bernard-Mantel, *J. Magn. Magn. Mater.* **520**, 167122 (2021).
- [53] M. Shen, Y. Zhang, W. Luo, L. You, and X. Yang, *J. Magn. Magn. Mater.* **485**, 69 (2019).